PAGE

Form Approved
OMB No. 0704-0188

1. AGENCY USE ONLY (Leave blank)	2. REPORT DATE	3. REPORT TYPE AND DATES COVERED
	March 1993	Professional Paper

4. TITLE AND SUBTITLE

TRIPLET STATES AND OPTICAL ABSORPTIONS IN FINITE POLYENES AND CONJUGATED POLYMERS

5. FUNDING NUMBERS

In House Funding

6. AUTHOR(S)

D. K. Campbell, J. T. Gammel, H. Q. Lin, E. Y. Loh, Jr.

7. PERFORMING ORGANIZATION NAME(S) AND ADDRESS(ES)

Naval Command, Control and Ocean Surveillance Center (NCCOSC)
RDT&E Division
San Diego, CA 92152–5001

8. PERFORMING ORGANIZATION REPORT NUMBER

9. SPONSORING/MONITORING AGENCY NAME(S) AND ADDRESS(ES)

Naval Command, Control and Ocean Surveillance Center (NCCOSC)
RDT&E Division
San Diego, CA 92152–5001

10. SPONSORING/MONITORING AGENCY REPORT NUMBER

11. SUPPLEMENTARY NOTES

12a. DISTRIBUTION/AVAILABILITY STATEMENT

Approved for public release; distribution is unlimited.

12b. DISTRIBUTION CODE

13. ABSTRACT (Maximum 200 words)

We study the nature of triplet states in correlated, quasi one dimensional bands, with emphasis on the half-filled case relevant to conducting polymers. To incorporate both electron-phonon and electron-electron interaction effects, we use a Peierls-extended Hubbard Hamiltonian, which we solve for finite systems via (numerically) exact diagonalization (Lanczos) techniques. We extend our results to polymers using both standard finite-size extrapolation techniques and a novel boundary condition averaging scheme. First, we examine the nature of the lowest triplet state, focusing on the crossover from the free electron picture of neutral soliton pairs to the strongly correlated limit of spin excitations. We then examine the optical absorption spectra corresponding to (allowed) triplet-triplet transitions; for this purpose it is important that our novel boundary condition averaging method maintains sharp gap-edge features while reducing spurious rapid frequency variations produced by the finite-size approximations to the band-to-band continuum. We compare our results to data on triplet transitions in finite polyenes and discuss possible additional experimental implications, including the interpretation of recent spin-dependent photomodulation (SDPM) experiments in both *trans-(CH)*$_x$ and non-degenerate ground state conjugated polymers.

Published in *Synthetic Metals*, Vol. 49-50, 1992, p 631.

14. SUBJECT TERMS			15. NUMBER OF PAGES
triplet-triplet transitions spin-dependent photomodulation (SDPM)	band-to-band continuum		16. PRICE CODE
17. SECURITY CLASSIFICATION OF REPORT	18. SECURITY CLASSIFICATION OF THIS PAGE	19. SECURITY CLASSIFICATION OF ABSTRACT	20. LIMITATION OF ABSTRACT
UNCLASSIFIED	UNCLASSIFIED	UNCLASSIFIED	SAME AS REPORT

21a. NAME OF RESPONSIBLE INDIVIDUAL	21b. TELEPHONE (Include Area Code)	21c. OFFICE SYMBOL
J. T. Gammel et al.	(619) 553-6576	Code 573

TRIPLET STATES AND OPTICAL ABSORPTIONS IN FINITE POLYENES AND CONJUGATED POLYMERS

David K. Campbell*, J. Tinka Gammel*,†, Hai-Qing Lin*, and E.Y. Loh, Jr.‡

*Center for Nonlinear Studies, MS-B258, Los Alamos National Laboratory, Los Alamos, NM 87545

† Naval Ocean Systems Center, San Diego, CA 92152

‡ Thinking Machines Corporation, 245 First Street, Cambridge, MA 02142-1214

December 6, 1991

Abstract

We study the nature of triplet states in correlated, quasi one dimensional bands, with emphasis on the half-filled case relevant to conducting polymers. To incorporate both electron-phonon and electron-electron interaction effects, we use a Peierls-extended Hubbard Hamiltonian, which we solve for finite systems via (numerically) exact diagonalization (Lanczös) techniques. We extend our results to polymers using both standard finite-size extrapolation techniques and a novel boundary condition averaging scheme. First, we examine the nature of the lowest triplet state, focusing on the crossover from the free electron picture of neutral soliton pairs to the strongly correlated limit of spin excitations. We then examine the optical absorption spectra corresponding to (allowed) triplet-triplet transitions; for this purpose it is important that our novel boundary condition averaging method maintains sharp gap-edge features while reducing spurious rapid frequency variations produced by the finite-size approximations to the band-to-band continuum. We compare our results to data on triplet transitions in finite polyenes and discuss possible additional experimental implications, including the interpretation of recent spin-dependent photomodulation (SDPM) experiments in both *trans*-$(CH)_x$ and non-degenerate ground state conjugated polymers.

I. Introduction

No interpretation of the excited state spectra and in particular of the dynamics of photoexcitations in finite polyenes and conducting polymers can be considered complete unless it correctly captures the important role of the triplet states. In (derivatives of) finite polyenes, triplet states are known to be of considerable importance in the processes of vision [1] and of photosynthesis [2], in that they control crucial relaxation paths after electronic excitation. In conducting polymers, triplets appear essential to understanding the nature of long-lived excited states and specifically of the spectra observed in photoinduced photoabsorption. From a theoretical perspective, knowledge of triplet states and their properties can provide additional insight into the relative importance of electron-electron (e-e) and electron-phonon (e-p) interactions and can help determine the parameters in the theoretical models of these materials.

Fortunately, a number of recent experimental results have begun to clarify the properties of triplet states, including the energy levels and their (linear) optical absorption properties. In finite polyenes, earlier work using pulse radiolysis and flash photolysis [1, 2] to observe the very weak (forbidden) singlet-triplet in addition to the (allowed) triplet-triplet transitions has be supplemented by the results of ultra high resolution spectroscopy [3] and of embedding the polyenes in " spectroscopic matrices" [4] which enhance the forbidden transitions. In conducting polymers, novel experimental techniques including "optically detected magnetic resonance" (ODMR) [5, 6, 7, 8], photcinduced ESR [9], and "spin-dependent photomodulation" (SDPM) [10, 11] have begun to produce definitive information on the locations and properties of triplet excitations.

Theoretical studies of triplets in these systems have to date been less extensive. Within the framework of the SSH model [12], Su [13] showed that the lowest triplet excitation was expected to be a pair of *neutral* solitons with aligned spins. Hartree-Fock [14], renormalization group [15, 16] and configuration interaction [17] studies have suggested that in models in which electron-electron interactions are present, triplets could play an especially important role as "constituents" in the covalent *singlet* excitations, such as the "celebrated" 2^1A_g state.

However, these intriguing pioneering studies have not been followed by definitive analyses which simultaneously (1) incorporate completely the full effects of the possible geometric relaxations of triplets and (2) solve *exactly* the true many-body problem that arises when e-e interactions are properly included. Our goal in the present article is to begin such a definitive analysis by studying via an exact many-body method a model which incorporates both e-p and e-e interactions of arbitrary strengths. We begin in Section II by introducing the Peierls-extended Hubbard model in the form appropriate for *trans*-polyacetylene (*trans*-$(CH)_x$) and discussing the numerical exact diagonalization (Lanczös) technique we use for solving the model. We also explain our "boundary condition averaging" method for extracting estimates of energies and other properties, which estimates are considerably less sensitive to finite size effects than those obtained by conventional means. In Section III we review the analytically tractable weak- (SSH model) and strong- (Heisenberg model) coupling limits and discuss the expectations for triplet properties in these limiting cases. Section IV contains the details of our numerical results

for the energies, geometries, and optical absorptions of both triplet and (for comparative purposes) singlet states. In Section V we examine the possible role of triplet states in recent spin-dependent photomodulation experiments and the relation of the triplet states to the (optically forbidden) 2^1A_g state. Finally, in Section VI we discuss a number of unresolved issues and future challenges for both theory and experiment.

II. The Peierls-Hubbard Model and Lanczös Method

In the context of conducting polymers, the one-dimensional Peierls-extended Hubbard Hamiltonian [18] provides a theoretical framework capable of treating both electron-phonon (e-p) and electron-electron (e-e) interactions of arbitrary strengths. In the specific case of *trans*-polyacetylene (*trans*-$(CH)_x$), the Hamiltonian is

$$H = \sum_\ell (-t_0 + \alpha\delta_\ell)B_{\ell,\ell+1} + \frac{1}{2}K\sum_\ell(\delta_\ell - a_0)^2 + \frac{1}{2M}\sum_\ell p_\ell^2 + U\sum_\ell n_{\ell\uparrow}n_{\ell\downarrow} + V\sum_\ell n_\ell n_{\ell+1} \ , \quad (1)$$

where $c^\dagger_{\ell\sigma}(c_{\ell\sigma})$ creates (annihilates) an electron in the Wannier orbital at site ℓ, $n_\ell = n_{\ell\uparrow} + n_{\ell\downarrow}$, where $n_{\ell\sigma} = c^\dagger_{\ell\sigma}c_{\ell\sigma}$, is the density operator, and $B_{\ell,\ell+1} = \sum_\sigma(c^\dagger_{\ell\ \sigma}c_{\ell+1\ \sigma} + c^\dagger_{\ell+1\ \sigma}c_{\ell\ \sigma})$ is the electron hopping operator, though it may also usefully be viewed as a "bond-charge" operator [19]. δ_ℓ represents the projection along the chain axis of the relative displacement between the (CH) units at sites ℓ and $\ell+1$ and p_ℓ the momentum of the (CH) unit at site ℓ and mass M. The single particle parameters of the model are the hopping integral t_0 for the uniform (CH) ionic lattice, the electron-phonon coupling α describing the modification of the hopping between adjacent sites due to the distortion of the underlying discrete lattice, and the lattice spring constant K representing the cost of distorting the lattice of $(CH)_x$ moieties due to interactions not otherwise explicitly included in the model, such as the core electron repulsion. Since in some of our calculations we shall be interested in the comparative geometries of the ground and excited states, rather that using the usual constraint $\sum_\ell \delta_\ell = 0$, we have defined a_0 to be the value needed in order that in the uniformly dimerized ground state the sum is zero. Using this value of a_0 allows to to determine the excited geometries in a manner consistent with that in the ground state. As in almost all studies of this model, we work in the adiabatic limit, ignoring the lattice momentum term in Eq. (1) and treating the lattice coordinates as classical variables whose values are determined by minimizing the electronic energy self-consistently.

The electronic many-body terms due to Coulomb repulsion are parameterized by the conventional Hubbard U and V, describing the on-site and nearest-neighbor interactions, respectively. In the limit $U = V = 0$ (dominant e-p interactions), Eq. (1) reduces to the familiar Su-Schrieffer-Heeger (SSH) model [12] of *trans*-$(CH)_x$. In the $\alpha = 0$ limit (no e-p but dominant e-e interactions), it reduces to the extended Hubbard model [19, 20].

Considerable experimental evidence (reviewed in [18]) suggests that parameter values appropriate for conducting polymers lie in the intermediate coupling regime: $U = 4t_0$, where $4t_0$ is the full single-particle bandwidth. To obtain definitive results in this parameter regime, one must use exact many-body techniques. We adopt adopt the Lanczös exact diagonalization technique, which we describe very briefly below because of some sig-

nificant modifications which simplify considerably the measurement of optical absorption spectra.

For studies of the optical transitions, we shall need the current operator

$$j_{\ell,\ell+1} = i(t_0 - \alpha\delta_\ell)\sum_\sigma (c^\dagger_{\ell+1\ \sigma} c_{\ell\sigma} - c^\dagger_{\ell\sigma} c_{\ell+1\ \sigma}) \quad . \tag{2}$$

The Fourier transform of $j_{\ell,\ell+1}$ is

$$J_q = \frac{1}{\sqrt{N}} \sum_\ell e^{-iq(\ell+\frac{1}{2})} j_{\ell,\ell+1} \quad . \tag{3}$$

The optical-absorption coefficient $\alpha(\omega)$ is given by

$$\alpha(\omega) = \frac{1}{\omega} \sum_m |\langle m|J_q|0\rangle|^2 \delta(\omega - (E_m - E_0)) \ . \tag{4}$$

In our variant of the Lanczös algorithm, we start generating the basis set by normalizing some trial wavefunction, which we typically express in terms of real space occupations. We have usually chosen to start from a *random* wavefunction, subject only to the constraint that $S_z = 0$, where S_z is the z-component of the total spin. Since the Hamiltonian contains no (net) spin flip operators, this constraint is preserved throughout the calculations. Choosing a random starting wavefunction does not cost much extra computing time in most cases and, importantly, statistically prevents one from picking a wavefunction with the wrong symmetry.

The Lanczös procedure is to generate the matrix elements of the Hamiltonian in a basis that is built up from this trial state. The basis is incremented one wavevector at a time by operating on the last basis state with the Hamiltonian and then orthonormalizing the product to all previous basis states. Notice that by construction $\langle j|H|i\rangle$ is tridiagonal [21, 22]. Within this basis, that linear combination of states with the lowest expected energy forms the estimate of the ground state. The basis will probably not be complete: we generally will truncate it when we have run out of computer memory, when the estimate of the ground-state energy stops dropping, or when the residual of a new state, after orthogonalizing to other components, is negligible.

Importantly, the calculations of optical absorption spectra — and hence also gaps, conductivities, and susceptibilities — are easily carried out by generating H in a suitable basis. For the optical absorption, we first calculate the ground state, $|\psi_0\rangle$ using the technique described above. We then generate a new basis, using $J_q|\psi_0\rangle$ as the first state and obtaining subsequent states by the application of H. Once the basis has been generated, the problem of calculating $\alpha(\omega)$ reduces to finding the spectral weight of this first state for the tridiagonal Hamiltonian. In essence, this amounts to determining the spectrum by measuring the moments of H^n and using the cumulant expansion.

The final theoretical ingredient in our analysis is somewhat technical and involves the use of a novel "boundary condition averaging" technique for effectively reducing the finite size corrections to optical gaps and spectra and thereby enhancing the convergence

of finite system results to those of the infinite system. Readers interested in the technical details should consult the original references [22, 23]. Here we note just that by "boundary condition averaging" we mean, for example, that the total energy of the system is viewed as the *average* of the energies derived separately for each of several boundary conditions:

$$E = \frac{1}{N_{bc}} \sum_{\{b.c.\}} x_{bc} E[b.c.] \tag{5}$$

where N_{bc} is the number of boundary conditions used and x_{bc} is a normalized weighting factor, which may depend on which quantity we are studying. Similarly, the optical absorption is viewed as the average of absorptions from the separate boundary conditions.

The value of the self-consistent adiabatic lattice distortion is found by minimizing the total energy

$$\partial E / \partial \delta_\ell = 0 \ . \tag{6}$$

At fixed K, to find the ground state lattice distortion we use the Lanczõs procedure iteratively to calculate the new guess at the minimum energy distortion from the expectation value of the bond charge: this is just the familiar "self-consistency condition"

$$K(\delta_\ell - \mathrm{a}) = -\alpha \langle B_{\ell,\ell+1} \rangle \tag{7}$$

with the proviso that it be appropriately averaged over the boundary conditions.

III. Analytic Limits

We can gain considerable insight into our later numerical results – as well as relate to earlier work in the literature – by considering the two essentially analytic limits of weak and strong coupling.

A. The Weak Coupling Limit

In accordance with the common usage, by the "weak-coupling" limit of the Peierls-extended Hubbard model we mean the case in which (e-e) interactions are weak, so that an independent particle model provides an accurate approximation. For $U = V = 0$, the Hamiltonian in Eq. (1) reduces to the SSH model [12], for which the solitonic nature of the triplet state has been established by Su [13]. We summarize briefly the results. Working in momentum space, one obtains the ground states of the singlet and triplet by filling the single particle (band theory) energy levels up to the Fermi surface. The singlet ground state corresponds to the occupancy shown in Fig. 1a, in which all levels below the (Peierls) band gap are filled. Momentarily ignoring relaxation of the lattice in the triplet state, we see that the lowest triplet would be as sketched in Fig. 1b, since two electrons of the same spin cannot share a single band state. Hence in this approximation the energy of the lowest triplet would be $E_T^0 = 2\Delta_0$, so that the triplet would occur at the same energy as the optical gap. However, as shown by Su [13], within the SSH model, the true lowest triplet state involves a relaxation of the lattice to form a pair of (widely

separated) neutral solitons (which is allowed topologically). Hence the schematic single particle energy levels are as shown in Fig. 2. The energy of this relaxed triplet, which is the true triplet ground state in the weak-coupling limit, is

$$E_T^R = E_{S^0 S^0} = \frac{(4\Delta_0)}{\pi}. \tag{8}$$

Thus the triplet lies below the optically allowed (^1B_u) state. Further, the geometry of the relaxed triplet state involves a soliton-antisoliton lattice distortion. Finally, the lowest triplet-triplet optical transition will involve promotion of one of the occupied midgap states into the conduction band and will thus occur at $\Delta_T = \Delta_0 = 1/2\Delta_S$, where we have denoted the singlet-singlet optical gap by Δ_S.

For later purposes, we note two specific features of this weak coupling limit. First, the role of "Jahn-Teller" and "anti-Jahn-Teller" systems is reversed between the singlet and triplet states: that is, the triplet states (in the absence of a gap) are degenerate at the Fermi surface for 4N + 2 systems with periodic (or 4 N anti-periodic) boundary conditions. This can affect the interpretation of numerical results on small-sized systems, at least for weak coupling. Second, for (forbidden) optical transitions between the singlet ground state and the triplet state – such as would be visible in the high resolution spectroscopy [3] or in the "spectroscopic matrices" [4] – one would expect to observe the *un*relaxed form of the triplet state because of the essentially instantaneous nature of the transition. However, for allowed triplet-triplet transitions – as seen in any of the photoinduced measurements – the relaxed triplet state should be play the role of the *initial* state.

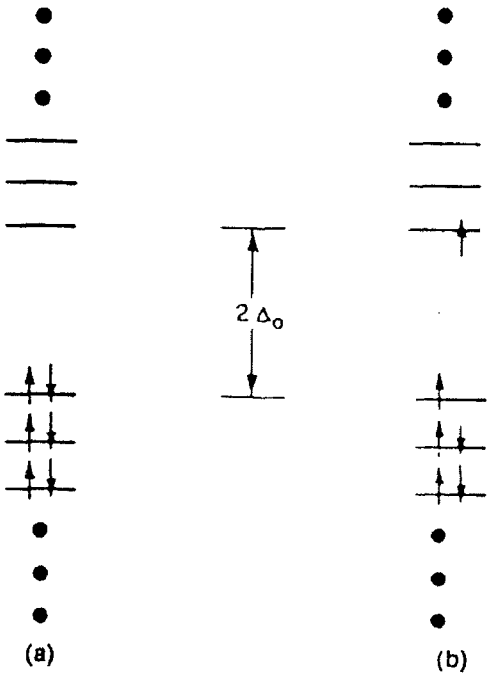

Figure 1 Caption: Schematic representations of the momentum space orbital occupancy for the *unrelaxed* (perfectly dimerized) (a) singlet and (b) triplet ground states. This situation is appropriate for the "weak coupling" ($U/t_0 = 0$) limit.

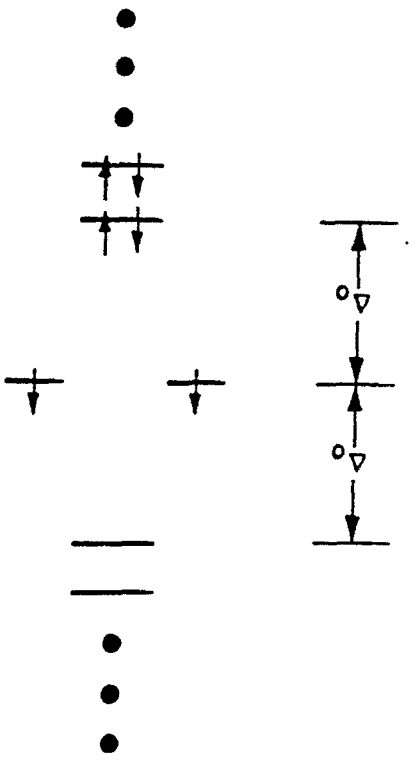

Figure 2 caption: Schematic representation of the momentum space orbital occupancy of the triplet ground state *after relaxation* of the lattice; the "two-soliton" lattice deformation leads to two mid-gap states, which are occupied as for two neutral solitons. This situation is appropriate for the "weak coupling" ($U/t_0 = 0$) limit.

B. The Strong Coupling Limit

We consider next the "strong coupling limit", by which we mean that the Coulomb interaction terms are much larger than all single particle energies. Working for simplicity with $V = 0$, this implies that $U/t_0 \rightarrow \infty$. Since in this limit there can be no doubly-occupied "sites" ($n_D = 0$), it is most natural to work in "real" (ie, coordinate) space and to use valence bond diagrams to describe the states. As is well known, in the absence of dimerization ($\alpha = 0$) the Hubbard model at half-filling in this limit becomes equivalent to an *antiferromagnetic* Heisenberg spin system, with effective coupling $J_{eff} \sim t_0^2/U$. Again we summarize briefly, using two figures, some familiar results (see, eg, [18] for a more detailed survey of results in this limit.)

In Fig. 3 we show schematic real space electron distributions for the singlet and triplet ground states in the strong coupling limit. In the singlet state, loosely speaking all the spins are aligned antiferromagnetically, whereas in the triplet state there are two bonds which are not antiferromagnetic: hence the energy of the triplet state in this limit is estimated to be $E_T \sim 2J_{eff} \sim t_0^2/U \rightarrow 0$. Strictly speaking, the Néel state shown in Fig. 3 a "cartoon", since the actual ground state can have only local (not long-range) spin order. However, for purposes of estimating energies, this naive picture is adequate.

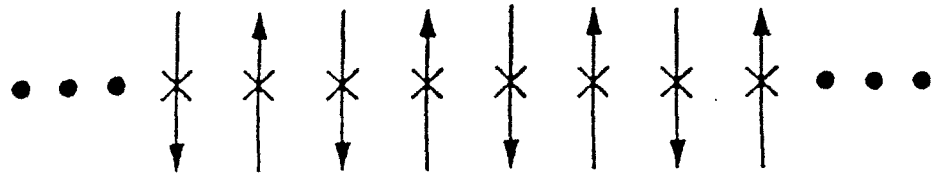

(a)

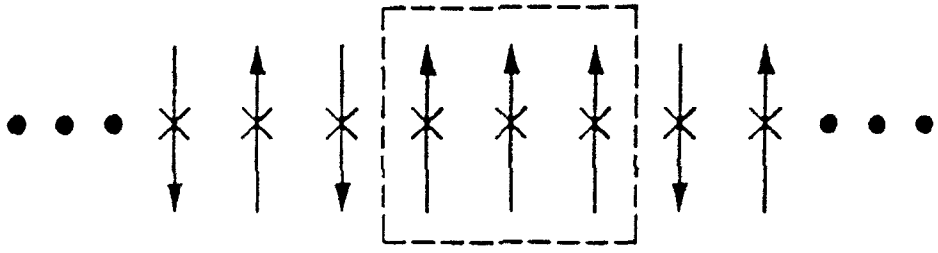

(b)

Figure 3 caption: Schematic representation of the distribution of electrons in *real space* in the "strong coupling" ($U/t_0 \rightarrow \infty$) limit. The Néel state shown is a cartoon; the actual ground state has only local (not long-range) order.

Figure 3 suggests that in the strong coupling limit the triplet state is a single localized excitation, in contrast to the weak coupling triplet, which is composed of two solitons. However, as shown schematically in Fig. 4, the particular real space configuration with three parallel spins adjacent to each other is in fact degenerate with (an infinite number of) other configurations in which two pairs of two parallel spins are separated by an arbitrary distance. Since these configurations are degenerate to leading order, the actual ground state will be a mixture of them. In the terminology of the Heisenberg spin system, the triplet state consists actually of *two* independent "domain walls", which must each therefore have spin 1/2. Note also that the "sense" of the antiferromagnetic ordering - ie, the $\pm(-1)^n$ - changes as one passes through one of the domain walls. In short, the strong coupling triplet (in the limit of zero dimerization) also consists of two independent excitations and when the e-p coupling is restored, we expect the geometry to reflect this. As noted above, the energy of the lowest triplet approaches zero, $E_T \sim 2J_{eff} \sim t_0^2/U \rightarrow 0$.

Further, the the triplet-triplet optical gap can readily be deduced by noting that the matrix element of the current operator (recall Eqns. (2)-(4)) in for both singlet-singlet and triplet-triplet transitions connects subspaces with $n_D = 0$ to those with $n_D = 1$ and thus involves an energy gap $\sim U$; hence $\Delta_T = \Delta_S \sim U$ in strong coupling.

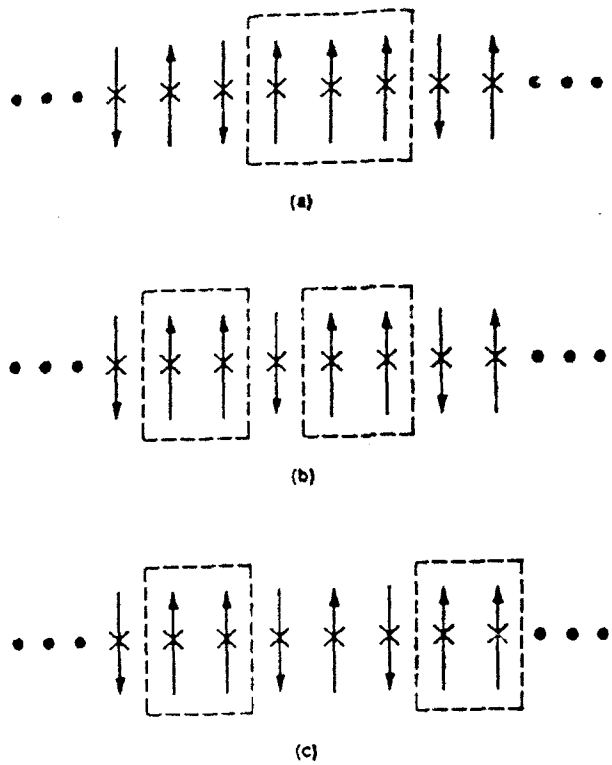

Figure 4 caption: Schematic representation of some of the degenerate real space electron distributions contributing to the triplet state in the "strong coupling" ($U/t_0 \rightarrow \infty$) limit. Note that each has (to leading order) energy $E_T = 2J_{eff} \sim t_0^2/U$

To explore the intermediate coupling regime and the crossover from weak to strong coupling, we turn in the following section to our Lanczös approach.

IV. Numerical Results

To discuss our numerical results we begin by defining in Fig. 5 the various observables we will study. As shown in that figure, these include singlet and triplet energies, optical gaps, and optical absorption spectra as functions of photon frequency. To organize our presentation, we divide it into three subsections covering energetics, geometries, and optical absorption.

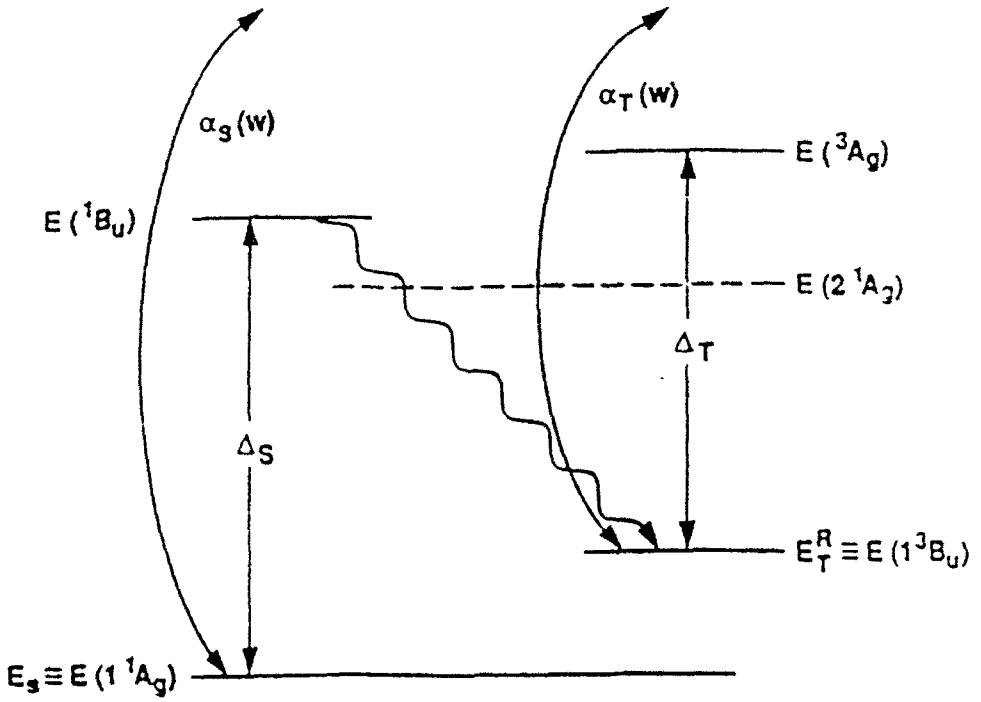

Figure 5 caption: Schematic diagram of the various energy levels and transition energies discussed in the text. Energy levels shown include the ground state energy ($E_S = E(1^1A_g)$), the first allowed singlet optical state energy ($E(^1B_u)$), the (relaxed lattice) triplet ground state energy ($E_T^R = E(1^3B_u)$), and the "second A_g" state energy ($E(2^1A_g)$). Transitions shown are the (allowed) singlet-singlet gap (Δ_S) and optical absorption coefficient ($\alpha_S(\omega)$) and the (allowed) triplet-triplet gap (Δ_T) and optical absorption coefficient ($\alpha_T(\omega)$).

A. Energetics

In Fig. 6 we plot the electronic contributions to the energies of the ground state and several important excited states as functions of the Hubbard U parameter; the states shown include the lowest triplet (1^3B_u), the second singlet "A_g" state (2^1A_g), and the "optical state" (2^1B_u). The figure is plotted for an eight site system with open boundary conditions, corresponding to (idealized) octatetraene. Note that the minimum value of U consistent with having the 2^1A_g below the 1^1B_u – as is observed in the longer finite polyenes [3] – is about 5 eV ($= 2t_0$). Our numerical results show that this "crossover" point is fairly insensitive to system size and to whether one works at fixed $\delta_{edge} = \delta$ or at fixed K. Note that over much of the range of U the energy of the 2^1A_g lies roughly twice as far above the ground state as does the 1^3B_u state; this strongly suggests that the 2^1A_g state is in some sense composed of two triplets, as indicated by the work of Tavan and Schulten [17].

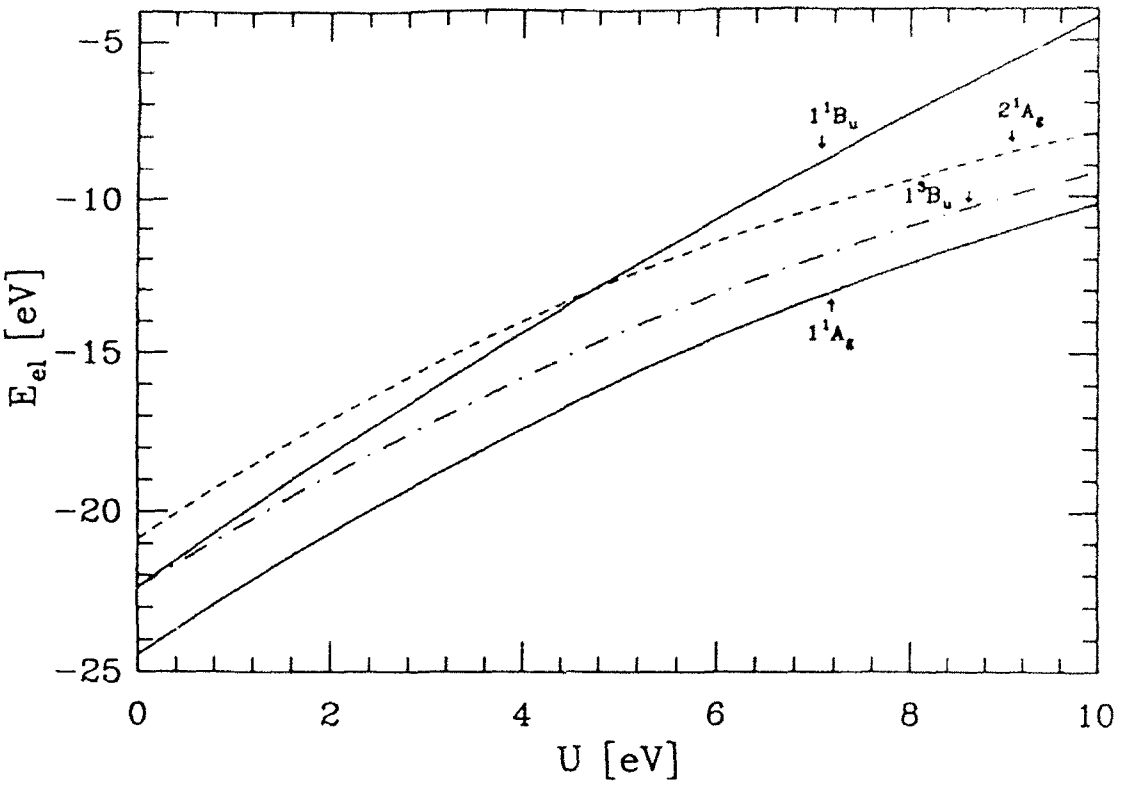

Figure 6 caption: Electronic contribution to the energies of the states 1^1A_g, 1^3B_u,2^1A_g, and 1^1B_u (optical gap) as functions of the Hubbard U. Other parameters are t_0=2.5eV, α = 4.1eVÅ, K = 51.1eV/Å^2, and V=0. Open chain boundary conditions on N=8 sites were used, and the geometry was constrained to be uniformly dimerized. Note these parameters give δ=0.03Åfor U=4eV, consistent with *trans*-polyacetylene. For these parameters, the 2^1A_g falls below the 1^1B_u near U=5eV.

B. Geometries

To study the geometries of the excited states, we consider both *constrained* structures – which are relevant to crystals of both finite polyenes and conjugated polymers in which solid state effects impose external forces on the individual chains (*e.g.* octatetraene, conjugated polymers in solid state) and *relaxed* structures, which are relevant to gas phase experiments on finite polyenes. In Fig. 7 we show the total energies – electronic plus lattice distortion – as functions of the (assumed constant !) dimensionless dimerization ($\alpha\delta/t_0$) for the four states plotted in Fig. 6. Two remarks concerning this figure are particularly significant. First, the constraint of constant dimerization (constrainted geometry) for the excited states is not realistic but is nonetheless useful for comparisons with other theoretical results, such as those obtained by Tavan and Schulten [17]. Second, the asymmetry between positive and negative values of the dimensionless dimerization arises simply because, for these finite systems with open boundary conditions, the negative values of $\alpha\delta/t_0$ correspond to systems with one fewer double bonds than the positive

values; these systems naturally have higher energies. The results shown in Fig. 7 are for $N = 8$ sites, but our results for $N = 10 - 14$ show very similar structure, suggesting little system size dependence in this result.

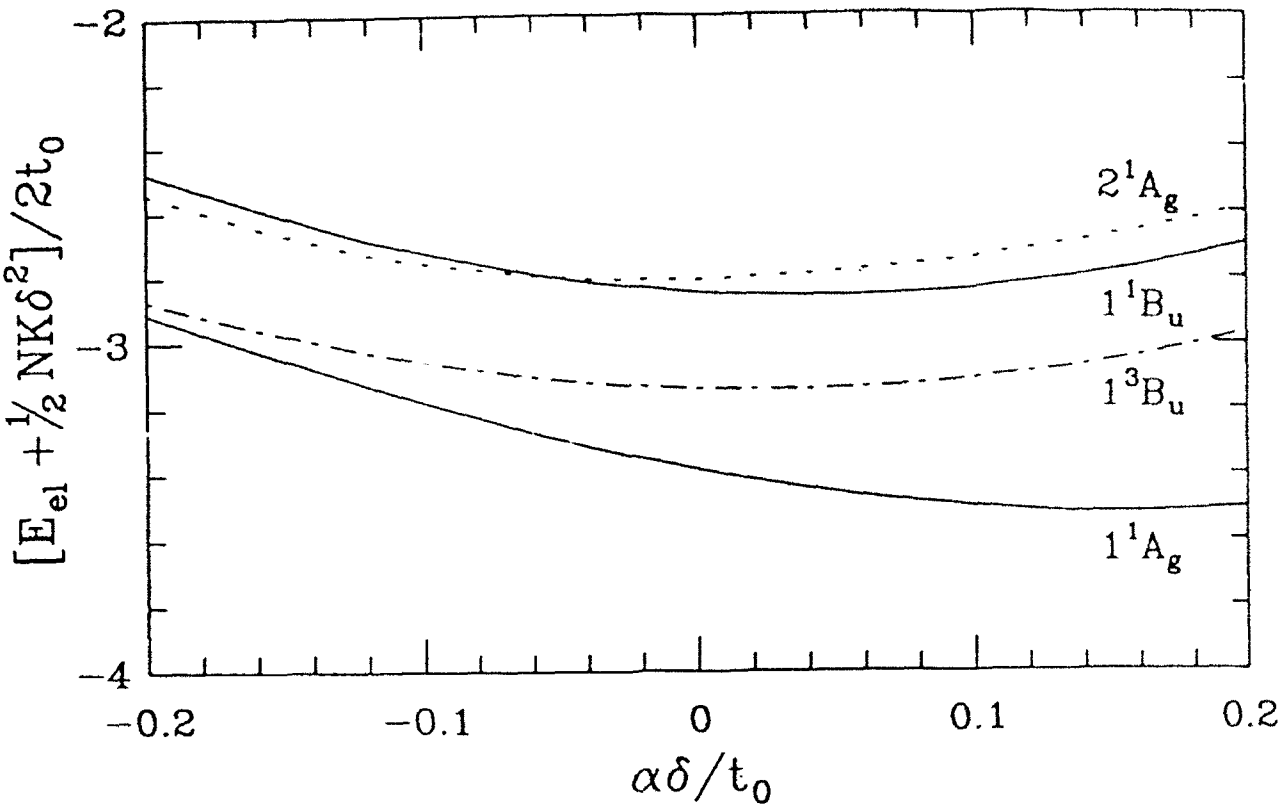

Figure 7 caption: Total energy as a function of the dimensionless dimerization $\alpha\delta/t_0$, showing the shift in the minimum value for various states of importance in optical experiments: 1^1A_g, 1^3B_u,2^1A_g, and 1^1B_u (optical gap). Parameters used are $U/2t_0$=0.8, $V/2t_0$=0, and $Kt_0/2\alpha^2$=2.0. Open chain boundary conditions (b.c.=0) on N=8 sites were used, and the geometry was constrained to be uniformly dimerized: see text

In Figs. 8 and 9 we show the relaxed geometries on open chains for the lowest singlet (Fig. 8) and triplet (Fig. 9) states. Note that the abscissa in each of these figures is the number of bonds, so that the total number ranges from 7 ($-3 \leq n \leq 3$) to 13 ($-6 \leq n \leq 6$). In Fig. 8, the otherwise uniform dimerization shows a slight increase at the ends; this is consistent with data on finite polyenes. In contrast, Fig. 9 shows substantial structure in the dimerization. In fact, in the large system sizes the lattice distortion is approaching that for a soliton pair. Thus it appears that even at intermediate (e-e) coupling, the solitonic nature of the triplet state – or at least of the lattice distortion corresponding to this state – remains.

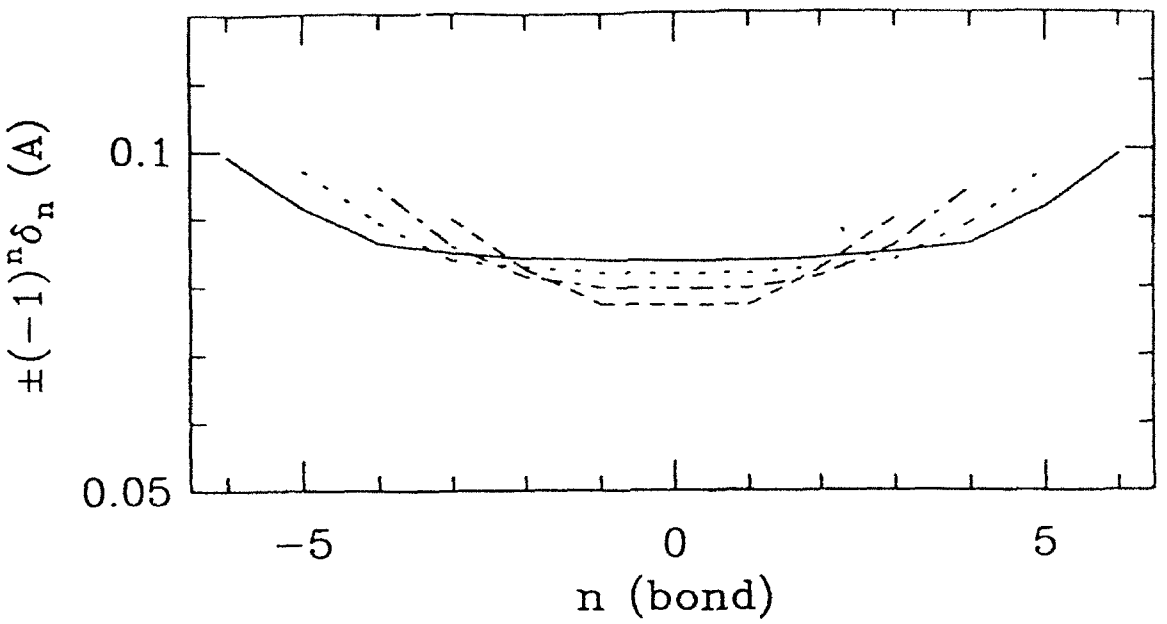

Figure 8 caption: The relaxed geometries of the ground state of open chains for systems containing between seven and thirteen double bonds, corresponding to finite polyenes from eight to fourteen (CH) units in the gas phase. Parameters are t_0=2.5eV, α = 4.1eV/Å, K = 22 − 24eV/Å, and V=0. Note that K was varied to eliminate the N dependence that arises when the dimerization is constrained to be uniform; when one allows relaxation via the small variation of K values, the remaining system size dependence is minimal.

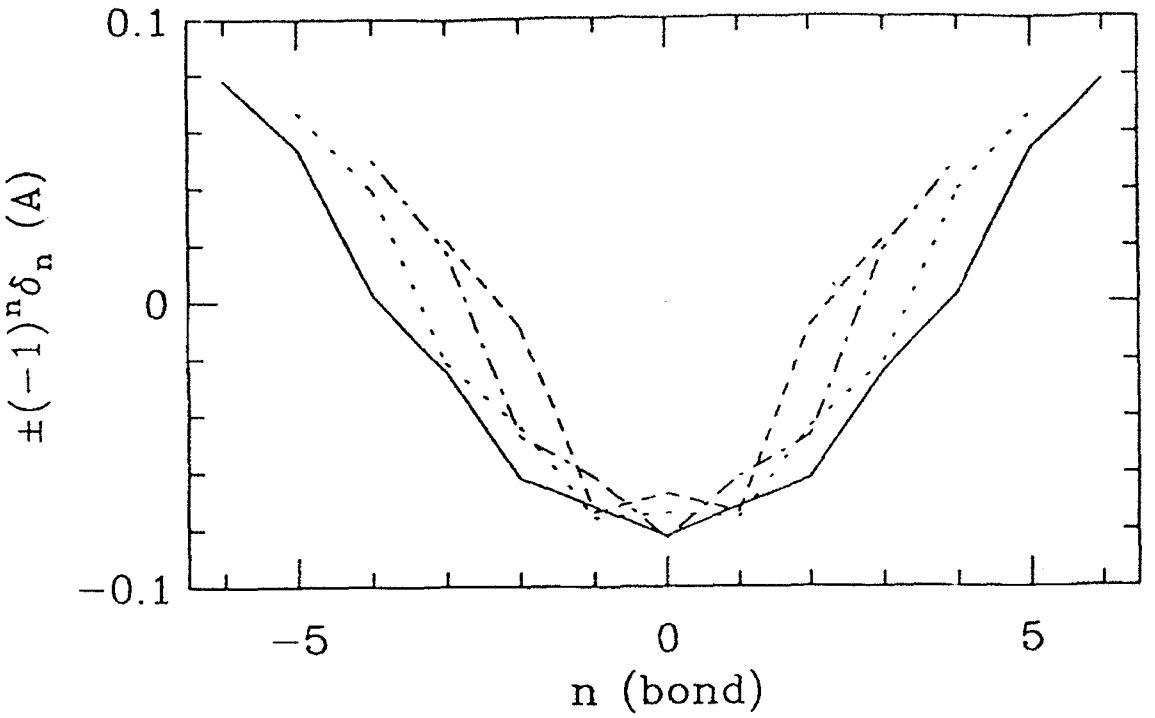

Figure 9 caption: The relaxed geometries of the lowest triplet state (13_u^B) on open chains for systems containing between seven and thirteen double bonds, corresponding to finite polyenes from eight to fourteen (CH) units in the gas phase. Parameters are same parameters as Fig. 8. Note the lattice distortion is approaching that for a soliton pair.

C. Optical Absorption

In discussing the optical absorptions, it is particularly important to distinguish between instantaneous "vertical transitions", either allowed or forbidden, and transitions to or from states with relaxed geometries, such as those occurring in photo-luminescence. In Fig. 10 we show various energy gaps – labeled generically by "Δ" in the figure – measured in optical experiments as functions of the Hubbard U. "n^1B_u" and "n^3A_g" are used to denote the "optically allowed" states, since for large U, the lowest states with non-zero optical absorption matrix elements are no longer the first states of these symmetries. For simplicity, we have plotted on the case with $V = 0$; hence there are no *excitonic* effects of the sort believed to be important in poly-diacetylene crystals [5].

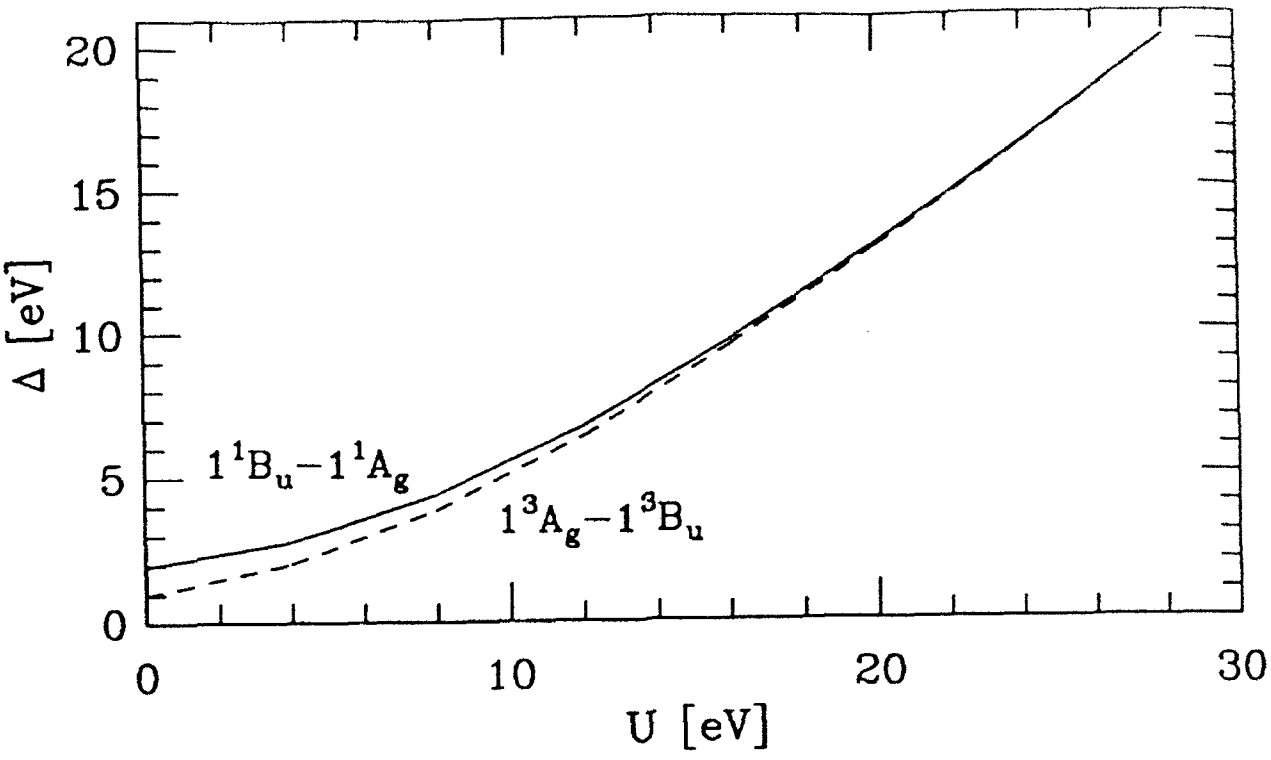

Figure 10 caption : Singlet-singlet (Δ_S) and triplet-triplet (Δ_T) energy gaps Δ measured in optical experiments as functions of Hubbard U. The parameters are t_0=2.5eV, $\alpha = 4.1\text{eV/Å}$, $K = 21.0\text{eV/Å}^2$, V=0, on an $N = 10$ site system, and antiperiodic boundary conditions were used.

We note that, as suggested by the analytic estimates in the weak and strong coupling limits, the allowed triplet-triplet gap (Δ_T) is always less than singlet-singlet gap (Δ_S). For $U = 0$ Δ_T is almost exactly half Δ_S (as predicted by weak coupling), while for large U, $\Delta_T \rightarrow \Delta_S$, as expected in strong coupling.

Finally, in Fig. 11 we plot the frequency dependent absorption coefficient , $\alpha(\omega)$, for both singlet-singlet (bottom curve, $\alpha_S(\omega)$) and triplet-triplet (middle curve, $\alpha_T(\omega)$) absorptions, as well as their difference (top curve). The largest peak in each case is at the edge of the optical gap, indicating that for these intermediate values of U the remnant of the one-dimensional single particle density-of-states peak survives in the optical absorption. The prominent higher feature in the singlet absorption has been identified previously [22] as a "decoupled dimer" peak: that is, a feature that arises because of the dimerization and which increases in intensity with increasing dimerization. This feature is less prominent in the triplet case because a triplet dimer has no allowed optical transitions, so that the presence of the single triplet on these small systems tends to reduce the intensity of this peak.

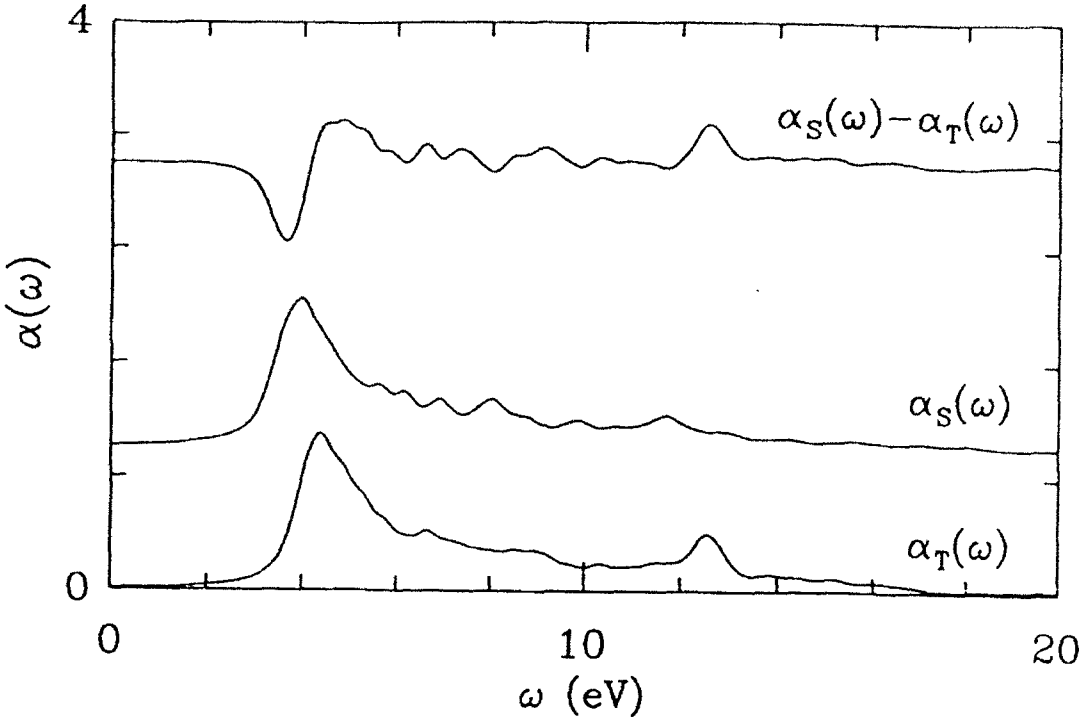

Figure 11 caption: The optical absorption coefficients as functions of frequency (ω) for allowed singlet-singlet transitions (called α_S in the text), allowed triplet-triplet transitions (called α_T in the text), and for the difference for an intermediate value of U (= 8 eV). Other parameters are as in Fig. 8. The spectra are averaged over boundary conditions (b.c.=-1,-0.5,0,0.5,1) *and* over system sizes N=8,10,12,14. The triplet and singlet absorptions were calculated using the relaxed geometry of the respective cases. The spectra are displaced for clarity and obtained from the raw data by Lorentzian broadening; this later procedure leaves some residual unphysical high frequency oscillations in the spectra. Note however the clear presence of the decoupled dimer peak in the singlet spectrum.

V. Application to Photoexcitations in Conjugated Polymers

A. The 2^1A_g and 1^3B_u states

In our discussion of the energetics of excited states (cf. Fig. 6), we noted that over much of the range of U the energy of the 2^1A_g lies roughly twice as far above the ground state as does the 1^3B_u state and remarked that this strongly hints that the 2^1A_g state is in some sense composed of two triplets, as suggested also by the work of Tavan and Schulten [17]. At the same time, from our studies of the geometries of excited states, we found that the 1^3B_u state had the lattice distortion appropriate to *two* neutral solitons (cf. Fig. 9). Does this mean that one should view the 2^1A_g state as composed of *four*

solitons? Such an interpretation was proposed in the renormalization group studies of Hayden and Mele [15, 16] but is explicitly contradicted in the configuration interaction studies [17] and (at least apparently) in combined experimental/theoretical studies on octatetraene [24]. Unfortunately, it is easier to argue why each of the purely theoretical studies could be incorrect than it is to determine a definitive answer to this question. In the renormalization group studies, the technique of constructing larger systems by combining smaller ones produces a natural bias against states with "long bonds" in the valence bond description (see [18] for a more thorough description of this effect). But these long bond states would correspond precisely to the A_g state made up of only two triplets, rather than four solitons. On the other hand, in the configuration interaction calculations, the geometries were not completely relaxed, so that one could argue that a bias existed against the formation of solitons. At present, our data on the *fully relaxed* geometry and energy of the 2^1A_g state on the largest systems (N = 12,14) are not sufficient to determine the resolution of this question unambiguously. This difficulty arises in part because the 2^1A_g state is not the lowest singlet state of A_g symmetry and thus must be extracted from the Lanczös data with considerable care.

B. Consistency with SDPM data

Recent studies of the spin dependent photomodulation (SDPM) [10, 11] in both degenerate ground state (*trans*-$(CH)_x$) and non-degenerate ground state polymers (PPV) identify the spins associated with long-lived excitations and assign the so-called "high energy" peak to triplet-triplet transitions associated respectively to neutral soliton pairs in *trans*-$(CH)_x$ and to (spinless) neutral bipolarons (composed of two triplets) in PPV. Although more detailed quantitative studies are required, our present results on triplet states and their relations to other excited states (such as the 2^1A_g state) are consistent with such an interpretation. If one assumes a relaxation mechanism which allows the optical ^1B_u state to cross over to the lower-lying 2^1A_g state, then one can take advantage of the schizophrenic nature of this later state to explain both types of high energy peak. In the degenerate ground state system the "reversed sense" ground state has the same energy, so that the long bond that characterizes the 2^1A_g state can be weak. Hence the two spins associated with this bond can interact independently with the magnetic field, giving rise to a spin 1/2 signal. In non-degenerate ground state polymers, the region spanned by the long bond must also span a region of reversed sense of the bond order. Since this is not equal in energy to true ground state, the "long-bond" can't be too long; hence one sees no spin 1/2 but only spinless or triplet signatures. However, until substantiated by detailed quantitative studies, such a theoretical interpretation remains speculative.

VI. Discussion and Open Issues

We have shown that studying Peierls-extended Hubbard models with Lanczós exact diagonalization techniques and boundary condition averaging methods, allows one to explore the properties of triplet states in both finite polyenes and conjugated polymers over the entire range of e-p and e-e couplings. Our results are consistent with the known analytic

limits. More extensive studies should provide detailed interpretations of data from real finite polyenes, both in gas and crystal phases, and also from conjugated polymers.

Apart from these more detailed studies, there are several additional open issues which we plan to address. First, we shall attempt to find a definitive resolution of the problem of the geometry of the 2^1A_g state. Second, we intend to investigate quantitatively the consequences of "confinement" –ie, the lack of ground state degeneracy – in conjugated polymers. Third, we propose to study the potential roles of possible charged triplet states in doped conjugated polymers. Finally, we plan to explore the manifold of higher spin magnetic states in these models and systems, in the hope that they may provide still further insight.

ACKNOWLEDGEMENTS

We are grateful to John Bronzan, Richard Friend, Bryan Kohler, Valy Vardeny, and especially Sumit Mazumdar for stimulating and valuable discussions. Computational support was provided by the Advanced Computing Laboratory and the Center for Nonlinear Studies at Los Alamos National Laboratory. JTG was supported by a National Research Council-NOSC Research Associateship.

References

[1] R.S. Becker, R.V. Bensasson, J. Lafferty, T.G. Truscott, and E.J. Land, "Triplet Excited States of Carbonyl-Containing Polyenes", J. Chem Soc. Faraday Transactions 2 **74**, 2246-2255 (1978).

[2] J. Lafferty, A.C. Roach, R.S. Sinclair, T. G. Truscott, and E. J. Land, "Absorption Spectra of Radical Ions of Polyenes of Biological Interest", J. Chem Soc Faraday Transactions 2 **73**, 416- 429 (1976.)

[3] B. E. Kohler, private communication.

[4] V. Ramamurthy, J.V. Caspar, D.R. Corbin, B.D. Schlyer, and A.H. Maki, "Triplet State Photophysics of Naphthalene and α,ω-Diphenylpolyenes Included in Heavy-Cation-Exchanged Zeolites" *J. Phys. Chem.* **94**, 3391 (1990).

[5] L. Robins, J. Orenstein, and R. Superfine, "Observation of the Triplet Excited State of a Conjugated Polymer Crystal", *Phys. Rev. Lett.* **56**, 1850-1853 (1986).

[6] L.S. Swanson, J. Shinar, and K. Yoshino, "Optically Detected Magnetic Resonance Study of Polaron and Triplet- Exciton Dynamics in Poly(3-Hexylthiophene) and Poly(3-Dodecylthiophene) Films and Solutions", *Phys. Rev. Lett.* **65**, 1140 (1990).

[7] L. S. Swanson *et al.*, "Triplet Polaronic Excitons in Conducting Polymers: An X Band ODMR Study", *Syn. Met.*, these proceedings.

[8] J. Shinar and L. S. Swanson, "Optically Detected Magnetic Resonance Studies of Conducting Polymers: An Overview", *Syn. Met.*, these proceedings.

[9] N.F. Colaneri, D.D.C. Bradley, R.H. Friend, P.L. Burn, A.B. Holmes, and C.W. Spangler, "Photoexcited States in Poly(p-phenylene vinylene): Comparison with trans, trans -distyrlbenzene, a model oligomer" Phys. Rev. B **42**. 11670-11681, (1990).

[10] X. Wei, B. C. Hess, Z. V. Vardeny, and F. Wudl, "Studies of Photoexcited States in Polyacetylene and Poly(paraphenylenevinylene) by Spin-Dependent Photomodulation: the case of Neutral Photoexcitations", Utah/UCSB preprint, 1991.

[11] X. Wei, B. C. Hess, Z. V. Vardeny, "Photoexcitation of Spin-States in Conducting Polymers Studied by the Spin-Dependent Photomodulation Technique" Utah, 1991.

[12] W.P. Su, J.R. Schrieffer, and A.J. Heeger, "Solitons in Polyacetylene", *Phys. Rev. Lett.* **42**, 1698-1701 (1979); "Soliton Excitations in Polyacetylene", *Phys. Rev. B* **22**, 2099-2111 (1980), Erratum *B***28** 1138 (1983).

[13] W. P. Su, "Triplet Solitonic Excitations in *trans*-Polyacetylene", *Phys. Rev. B.* **34**, 2988-2990 (1986).

[14] H. Hayashi and K. Nasu, "Effect of Correlation on the Ground State, the singlet-exciton states, and the triplet-exciton states of trans-Polyacetylene", *Phys. Rev. B* **32**, 5295-5302 (1985).

[15] G. W. Hayden and E. J. Mele, "Renormalization Group Studies of the Hubbard-Peierls Hamiltonian for Finite Polyenes", *Phys. Rev. B.* **32**, 6527-6530 (1985).

[16] G. W. Hayden and E. J. Mele, "Correlation Effects and Excited States in Conjugated Polymers", *Phys. Rev. B.* **34**, 5484-5497 (1986).

[17] P. Tavan and K. Schulten, "Electronic Excitations in Finite and Infinite Polyenes", *Phys. Rev. B* **36**, 4337-4358 (1987).

[18] A survey of the Peierls-extended Hubbard model and its applications to conducting polymers is given in D. Baerisywl. D. K. Campbell, and S. Mazumdar, "An Overview of the Theory of Π-Conjugated Polymers", in *Conducting Polymers*, H. Kiess (ed) (Springer, 1991).

[19] D.K. Campbell, J. Tinka Gammel, and E.Y. Loh, Jr.,. "Modeling Electron-Electron Interactions in Reduced-Dimensional Materials: Bond-Charge Repulsion and Dimerization in Peierls-Hubbard Models", *Phys. Rev. B* **42** 475-492 (1990).

[20] J. Hubbard, "Electron Correlations in Narrow Energy Bands" *Proc. Roy. Soc. (London) A* **276** 238 (1963).

[21] See, *e.g.*, the section on Lanczös diagonalization in S. Pissanetsky, *Sparse Matrix Technology*, (Academic, 1984).

[22] E. Y. Loh, Jr. and D. K. Campbell, "Optical Absorption in Extended Peierls Hubbard Models", *Syn. Met.* **27** A499-A508 (1988).

[23] D. K. Campbell, J. Tinka Gammel, and E. Y. Loh, Jr., "Strongly Correlated Quasi One Dimensional Bands: Ground States, Optical Absorption, and Phonons", *Int. J. Mod. Phys B* **3**, 405-422 (1989).

[24] M. Aoyagi, I. Ohmine, and B.E. Kohler, "Frequency Increase of the $C = Ca_g$ Stretch Mode of Polyenes in the 2^1A_g State: *Ab Initio* MCSCF Study of Butadiene, Hexatriene, and Octatetraene", *J. Phys. Chem.* **94**, 3922 (1990).